Jpn. J. Appl. Phys. Vol. 42 (2003) pp. 4799–4803
Part 1, No. 7B, July 2003


# Characterization of Domain Ordering in Polymer and Dendrimer Thin Films Using Photoluminescence and Third Harmonic Generation (THG) Near-field Scanning Optical Microscopy (NSOM)

Richard D. SCHALLER, Lynn F. LEE, Thuc-Quyen NGUYEN[1], Preston T. SNEE and Richard J. SAYKALLY*

*Department of Chemistry, University of California, Berkeley, CA 94720-1460, U.S.A.*
[1]*Department of Chemistry and Biochemistry, University of California, Los Angeles, CA 90095-1569, U.S.A.*

(Received February 27, 2003; accepted for publication April 1, 2003)

We have utilized the high spatial resolution of near-field scanning optical microscopy (NSOM) to characterize nanoscopic electronic inhomogeneity in as-cast thin films of a light-harvesting dendrimer consisting of coumarin-343 (core) and coumarin-2 (peripheral) chromophores and in thermally annealed thin films of the semiconductive polymer poly(2-methoxy-5-(2′-ethylhexyloxy)-1,4-phenylene vinylene) (MEH-PPV). Using photoluminescence (PL) and third harmonic generation (THG) NSOM techniques, we have observed nanoscopic domains in these films that exhibit increased delocalization in the excited (using PL) and ground states (using THG). In addition, we have developed a procedure for examining NSOM images via calculation of radial distribution functions (RDFs). RDF analysis of the PL and THG NSOM images indicates that the domains exhibit correlated structure in annealed MEH-PPV films while the light-harvesting dendrimeric material does not. The existence or absence of such nanoscopic amorphous structure can be understood in terms of the molecular structure of each material. [DOI: 10.1143/JJAP.42.4799]

KEYWORDS: polymer, dendrimer, microscopy, nonlinear optics, domains, thin films, near-field, semiconductor, harmonic generation, photoluminescence

## 1. Introduction

There is much current interest in films of organic semiconductive polymers and dendrimeric materials for use in sensors, light emitting diodes, displays, and solar cells.[1–4] Significant impediments to effective incorporation of such materials into functional devices has been due to the introduction of inhomogeneity within the films as well as due to changes in material electronic properties, in comparison to solution phase characteristics, that occurs upon casting and processing of thin films. Near-field scanning optical microscopy (NSOM) has found widespread applicability to the study of thin film properties and heterogeneity. In the following work, we present results of NSOM studies of such samples and discuss a novel technique of applying radial distribution function (RDF) analysis to NSOM images to characterize their heterogeneity.

While NSOM does not at present afford spatial resolution that is as high as that which can be obtained with atomic force microscopy (AFM) and scanning tunneling microscopy (STM), NSOM is a particularly useful scanned probe technique for spectroscopic sample characterization.[5] Spatially resolved spectroscopic information affords a wealth of chemical information about a sample that is not obtainable with AFM or STM. Additionally, the integration of an increasing number of spectroscopic probes in combination with NSOM[5–14] provides access to an ever-wider variety of chemical information with nanoscale spatial resolution.

In recent studies, we have utilized spatially- and spectrally-resolved photoluminescence (PL) NSOM to observe and characterize domains of interchromophoric species in thin films of first- to fourth-generation (G1 to G4) light-harvesting dendrimers consisting of a coumarin-343 (C-343) core chromophore and coumarin-2 (C-2) peripheral chromophores,[15] and in films of poly(2-methoxy-5-(2′-ethylhexyloxy)-1,4-phenylene vinylene) (MEH-PPV), a highly processible form of PPV.[16,17] For each sample, we have been able to discern that the domains result from interchromophoric coupling because emission from these regions is red-shifted in comparison to spatially homogeneous regions of the films, which is characteristic of excimers or exciplexes.

While PL NSOM is very useful for the study of film emission properties, it is not sensitive to non-emissive chromophores. However, other optical techniques, such as third harmonic generation (THG)[18,19] can be combined with NSOM to directly probe ground state electronic inhomogeneity within films. We have developed[6,20] and utilized[21] THG NSOM as a sensitive probe of film electronic properties and inhomogeneity. THG NSOM is particularly sensitive to the presence of film domains that exhibit new absorption features such as MEH-PPV aggregates.[21–23] Furthermore, THG is a low background measurement, as is PL, and THG signals can be greatly enhanced when the photon energies involved in the process become degenerate with a transition frequency in the material giving rise to strong optical contrast.[18,19] Our spatially- and spectrally-resolved THG NSOM studies of MEH-PPV show that aggregation domains form upon thermal annealing of the film, a common processing step that often improves device performance.[22,24]

Below, we present PL NSOM images of a first-generation (G1) light-harvesting dendrimer film and THG NSOM images of a thermally annealed MEH-PPV film. Using a digital filtering technique, we perform radial distribution function (RDF) analysis of the NSOM optical data. This analysis shows that defined spatial relationships exist between aggregation domains in annealed MEH-PPV films while such structure is not observed in the less spatially extended dendrimeric film.

*To whom correspondence should be addressed.
E-mail: saykally@uclink4.berkeley.edu

## 2. Experiment

A commercial NSOM system (TMmicroscopes Lumina), equipped with a shear-force, tuning fork feedback system was employed for all presented near-field measurements. Chemically-etched fiber optic probes with a ~50 nm diameter tip were fabricated according to standard methods[25] and were mounted on 100 kHz tuning forks. A constant gap of ~5 nm between the tip and the sample surface was maintained throughout each scan. Topographical and optical signals were obtained simultaneously for comparison. Forward and reverse motions of the sample were collected as separate images as a check of image reproducibility and repeatable optical images were then added together to reduce random noise.

For PL NSOM measurements, a cw HeCd laser (Melles Griot) operating at 325 nm (attenuated to 5 μW) was used for sample excitation. For THG measurements, which require high laser peak powers in order to be observable, an amplified titanium:sapphire laser (800 nm, 80 fs, 1 kHz) (Spectra-Physics), made tunable in the near-IR with an optical parametric generator, was used for sample excitation following attenuation to ~700 μW. In both experiments, the laser was incident upon the sample in an oblique collection mode geometry as shown in Fig. 1. Photons produced by the sample were collected by the NSOM probe and could be directed to filters and a photomultiplier tube (PMT) for imaging or to a spectrograph and CCD to collect PL spectra. For all measurements, the NSOM probe was fixed while the sample was scanned in order to maintain a more constant tip/field geometry. Presented images are 200 × 200 pixel *x*-*y* arrays. In order to reduce effects of photo-oxidation, the entire NSOM apparatus was placed inside a sealed box that was purged with nitrogen gas continuously throughout all measurements.

Thin films (200 nm thickness for both materials) were prepared by spin-casting under a nitrogen atmosphere.

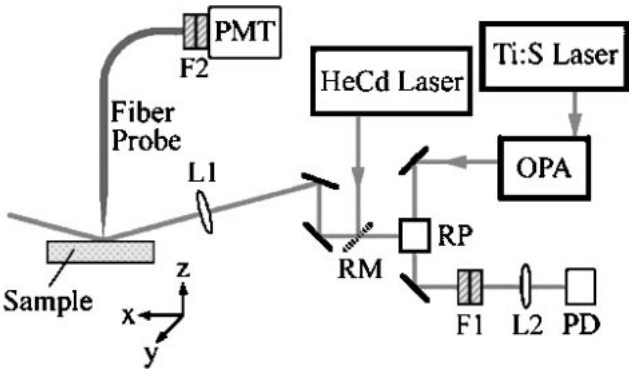


Fig. 1. Experimental Setup. Optical parametric amplifier (OPA); Rochon prism (RP); filters (F1-2); lenses (L1-2); removable mirror (RM); Ge photodiode (PD). PL NSOM experiments used a HeCd laser for cw sample excitation at 325 nm. THG NSOM experiments utilized an amplified, femtosecond pulsewidth laser system and OPA. Signal and idler wavelengths produced in the OPA were separated by a RP. The idler was used to produce the third harmonic while the signal was monitored with a PD to normalize for shot to shot laser fluctuations. Photons collected by the near-field probe were directed to filters and a photomultiplier tube (PMT) detector, which could be replaced with a 0.3 m spectrograph and back-illuminated, liquid nitrogen-cooled CCD to energy resolve collected photons.

Dendrimer films were cast from dichloromethane and MEH-PPV films were cast from chlorobenzene. Thermally annealed films of MEH-PPV were produced by heating the films above the glass transition temperature (~205°C) for several hours under the inert nitrogen atmosphere.[22]

## 3. Results and Discussion

Figure 2(b) shows a PL NSOM image collected at emission wavelengths >600 nm and the corresponding topography (shown in 2(b)) measured for a $(5\,\mu m)^2$ area of a thin film of the above-described G1 light-harvesting dendrimer. The topographical image, Fig. 2(c), shows many small bumps (average height ~20 nm) on the film surface. Many small (~350 nm diameter), circular, optically bright regions are also observed in the PL NSOM image. Although some of these bright regions correlate with topographical bumps, others do not. By spectrally resolving the collected emission from optically bright or dark regions regions, shown in Fig. 2(d), we have found that the domains are not simply related to the film thickness or surface topography, but exhibit increased emission in the red portion of the PL spectrum.[15] In similarity to our previous measurements of as-cast MEH-PPV films,[16] these PL domains are only observed when emission wavelengths that are red-shifted, in comparison to the spatially homogeneous regions of the film, are selectively detected.[15]

For this light harvesting dendrimer, photons at 325 nm selectively excite the C-2 peripheral chromophores, which then, due to significant spectral overlap, efficiently transfer energy to the C-343 core chromophore.[26] The isolated core chromophore subsequently emits a photon with an emission maximum in G1 films near 570 nm. However, the C-343 chromophores can also form interchromophoric species, such as C-343 excimers, which then, being more delocalized than the isolated core, become the lowest energy species and emit photons that are red-shifted.[15] Similar effects have been observed for another dendrimer system that have also been assigned to interchromophoric species formation at low dendrimer generation.[27,28] To be observed as domains, the nucleation of an excimer must promote the formation of additional interchromophoric species. In low generation films, the C-343 core chromophores are not significantly sterically isolated from interaction with other core chromophores. As the generation of the dendrimer is increased, we have observed that such red-shifted domains occur with an exponentially decreasing frequency per unit area and are only rarely observed in G4 dendrimer films.[15]

Shown in Figs. 3(a)–3(b) are THG NSOM images of a topographically featureless (topography not shown), thermally annealed film of MEH-PPV produced at $3\omega = 650$ nm using (a) *p*- and (b) *s*-incident fundamental ($\omega = 1.95\,\mu m$) laser polarization. Each image was produced for the same $(4.25\,\mu m)^2$ film area. For each THG NSOM image, many small (~150–300 nm minor diameter), ellipsoidal-shaped (~3 : 1 aspect ratio), optically bright regions are observed. Comparison of parts (a) and (b) shows that the spatial location of observed domains is dependent upon the excitation laser polarization.

We have previously shown that these THG-bright domains are not observed in any significant frequency prior to thermal annealing, nor are they detected when THG NSOM

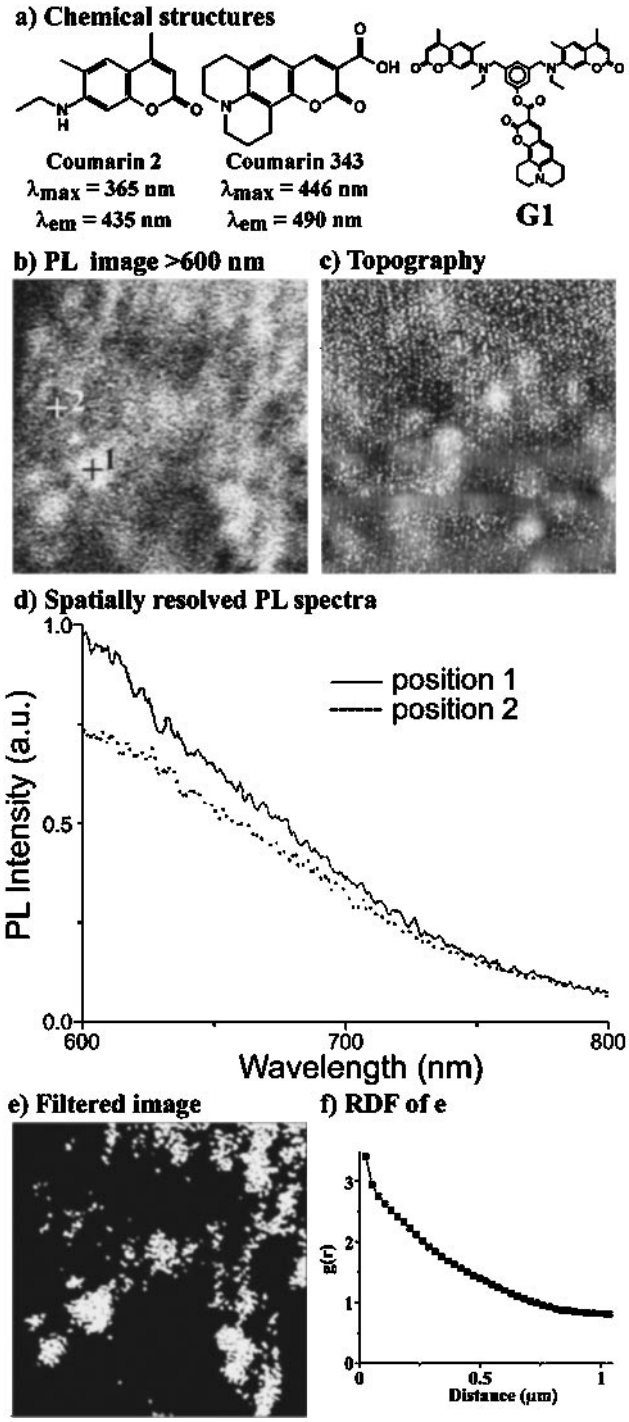


Fig. 2. (a) Chemical structures of coumarin-2, coumarin-343, and the first generation (G1) dendrimer studied in this work. (b) Photoluminescence (collected at wavelengths >600 nm resulting from excitation at 325 nm) and (c) surface topography NSOM images of the same $(5\,\mu m)^2$ area of a G1 dendrimer film. Many brighter-than-background regions are observed in the PL image. (d) PL NSOM spectra collected from the positions indicated in (b) exhibit different intensities in the red-tail of the emission. (e) A digitized representation of the PL NSOM image shown in (b) produced as described in the text was used to calculate the RDF for domains in the film. (f) The calculated RDF of the dendrimer film PL image shown in (e) shows very little structure and decays at longer distances to a value near 1, indicating that there is no mathematical spatial correlation between red-emitting domains in the film.

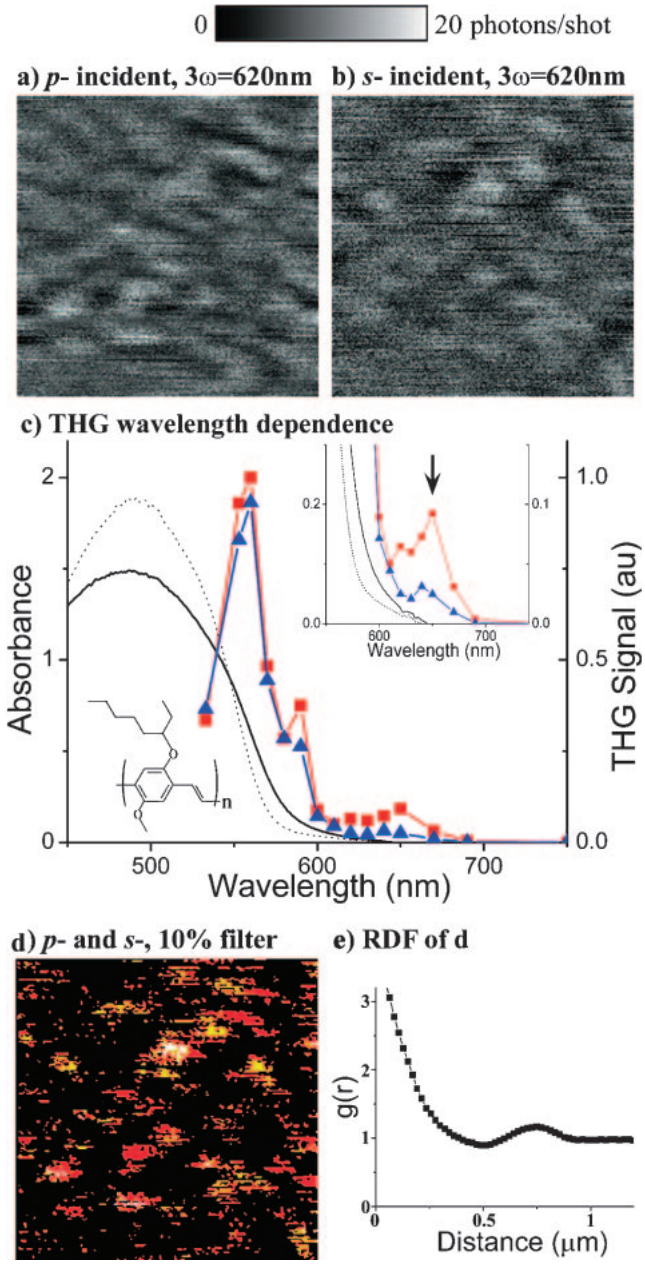


Fig. 3. Third harmonic generation NSOM images produced using 80 fs, 1.95 μm laser excitation pulses ($3\omega$ detected at 650 nm) with either (a) *p*- or (b) *s*-incident laser polarization collected from the same $(4.25\,\mu m)^2$ area of a thermally annealed MEH-PPV film. The surface topography for this area is featureless (flat to within ~2 nm) and is not shown. Many distinct THG-bright, ellipsoidal shaped regions are observed for each excitation laser polarization. Part (c) displays the linear absorption spectra of an as-cast (dotted line) and thermally annealed film (solid line) as well as the wavelength-dependent THG response of an annealed film THG-bright region (squares) and THG-dark region (triangles). The structure of MEH-PPV is shown as an inset. An arrow highlights the wavelength at which the THG NSOM images were produced. (d) A combined representation of the THG NSOM images shown in parts (a) and (b) was produced as described in the text and used for RDF calculations. Black represents pixels that are below a comparison voltage threshold for either incident laser polarization and red, yellow and white indicate pixels that are above threshold for *p*-, *s*-, and for both *p*- and *s*-incident laser polarizations, respectively. Less than 3% of the THG-bright domains were observed for both incident laser polarizations (shown in white). (e) The calculated RDF of the filtered THG NSOM image shown in (d) exhibits spatial correlation between domains at a distance of ~750 nm.

experiments are conducted at wavelengths that are degenerate with the absorption band of as-cast MEH-PPV films.[21] Furthermore, such domains were not observed using PL NSOM techniques. These observations taken together, also based upon the work of Nguyen *et al.*,[22,23] lead us to the conclusion that the THG NSOM images reveal the spatial location of aggregate domains which form upon thermal annealing of MEH-PPV films. These domains relax primarily through non-radiative pathways and exhibit red-shifted absorption features relative to the non-aggregated chromophores that result in resonant enhancement of the THG. The weak new absorption features result from very close packing of the polymer chains, which leads to ground state overlap of wavefunctions. It is also reasonable to infer, based upon previous THG experiments conducted on aromatic polymers,[29] that distinct domains are highlighted by the different incident laser polarizations due to the gross alignment of the polymer chains comprising the domains.[21]

To further analyze the optical images, we performed RDF analysis. RDF analysis is a useful treatment of the data, as it should allow us to detect any nanoscopic spatial correlation between the optically detected domains that we have observed. To analyze the images, we first digitally filter the 2-D matrix of detector voltage levels via comparison to a threshold value. Values in the matrix above or below this value are then set to one or zero, respectively. A two-color (digitized) representation of the optical image is next generated and compared to the original optical image. The threshold value is then adjusted until the digital image primarily highlights brighter regions in the film. Next, the probability as a function of distance ($g(r)$) of finding other above threshold pixels is calculated.

Calculated RDFs of the digitally filtered images shown in Figs. 2(e) and 3(d) are displayed in Figs. 2(f) and 3(e), respectively. We observe some similarities between the RDFs of the different films. At short distances from above threshold pixels $g(r)$ decreases rapidly from large values, and approaches unity at longer distances. The initially large values of $g(r)$ signify that an optically bright pixel is frequently proximal to other such pixels, which simply indicates that the majority of above threshold pixels are in the form of domains. Also, at longer range, the probability of finding other bright pixels becomes random and $g(r)$ approaches unity.

The RDF calculated for the PL NSOM image of the G1 dendrimer film looks very unstructured; $g(r)$ decreases from initially large values at short range and approaches unity at longer distances. The circularly averaged interchromophoric domain size is reflected in the distance over which $g(r)$ remains above 1. The RDF calculated for the thermally annealed MEH-PPV film, however, exhibits amorphous structure; following the initial decrease of $g(r)$ representing the circularly averaged aggregate domain size, the probability of observing other above threshold pixels increases at a distance of $\sim$750 nm before approaching a random probability at longer distances.

The observed differences between the calculated RDFs for these two aromatic 1- and 2-D organic materials merits discussion. The size and frequency of occurrence of domains in either material should be governed by dimensional frustration, in which growth is limited by the difficulty of fitting together in 3-D space the sterically bulky peripheral chromophores (for the dendrimer) or solublizing groups (for the polymer) of the molecules that are drawn together by the attractive forces involved in forming the more delocalized interchromophoric species, and/or by nucleation and growth, in which the presence of defects halts growth. Growth of domains will stop when the steric repulsion of packing together the peripheral or solublizing groups overcomes the driving force of formation. Because the dendrimer and polymer molecules differ with respect to both their steric bulk and their driving force for interchromophoric species formation, distinct packing of chromophores in the domains is expected. For a polymer similar to MEH-PPV, Teetsov *et al.* have found that modification of the polymer solublizing groups directly affects the size and electronic properties of the interchromophoric domains formed upon thermal annealing.[30] In the dendrimeric sample, we also observe that the frequency of domains decreases as the dendrimer generation is increased.[15] Domain growth in the polymer films can also be halted due to the presence of defect sites along the polymer aromatic backbone that result in poor chromophore packing. The dendrimer molecules, however, do not have such intrinsic defects, and therefore, dendrimer domains are likely to be governed principally by dimensional frustration.

Another distinction between the domains formed in these two materials, as seen in the polarized THG NSOM results, is that polymer chains in the aggregate domains are aligned, which presumably results from the high aspect-ratio shape of the individual MEH-PPV chromophores that are several repeat units long. In fact, the polymer chains must be well aligned in order to achieve significant overlap of wavefunctions in the ground state aggregate domain. It is conceivable that this alignment requirement gives rise to the large distance over which domain correlation is observed; domains that closely approach each other may be suppressed from aligning well and developing new ground state absorption features. Dendrimers, being more compact, are not likely to form domains with such ordering requirements.

Film processing conditions also certainly affect the properties of the observed domains.[31] The dendrimer films were produced by spin-casting, whereas MEH-PPV films were spin-cast and subsequently annealed thermally. Rapid evaporation of solvent during the casting process results in a kinetic freezing of the interchromophoric species that may have been present in solution,[16] which causes the domains to be positioned in the film with random spatial relationships. By thermally annealing the MEH-PPV films, the polymers are able to lower their thermodynamic energy in the very high polymer concentration of the film, resulting in the observed, tightly packed, spatially correlated, aggregate domains. Differences in the correlation between domains for the two films may then result from the processing step. We are at present, studying the effects of thermal annealing on interchromophoric domains in dendrimer films.

## 4. Conclusions

We have detected and characterized electronic inhomogeneities in thin films of a light harvesting dendrimer and a highly processible organic semiconducting polymer, MEH-

PPV, using linear and nonlinear optical NSOM techniques. RDF analysis of the optical data indicates that domains formed in the dendrimer film, observed using PL NSOM, occur randomly whereas aggregate domains observed by THG NSOM in annealed films of MEH-PPV form with some mathematical correlation. We propose that the differences in the amorphous structure of the two films are related to the differences in the shape of the molecules comprising the films and hence the structures of the domains themselves, as well as due to the film processing conditions.

## Acknowledgements

This work was supported by the Experimental Physical Chemistry Division of the National Science Foundation. We would like to thank Benjamin J. Schwartz, Jean M. J. Frechet, Alex Adronov and Louis H. Haber for their significant contributions to this work.

1) A. J. Lovinger and L. J. Rothberg: J. Mater. Res. **11** (1996) 1581.
2) R. H. Friend, R. W. Gymer, A. B. Holmes, J. H. Burroughes, R. N. Marks, C. Taliani, D. D. C. Bradley, D. A. Dos Santos, J. L. Bredas, M. Logdlund and W. R. Salaneck: Nature **397** (1999) 121.
3) S. K. Grayson and J. M. J. Frechet: Chem. Rev. **101** (2001) 3819.
4) C. C. Kwok and M. S. Wong: Macromol. **34** (2001) 6821.
5) M. A. Paesler and P. J. Moyer: *Near-field Optics: Theory, Instrumentation, and Applications* (Wiley, New York, 1996).
6) R. D. Schaller, J. C. Johnson, K. R. Wilson, L. F. Lee, L. H. Haber and R. J. Saykally: J. Phys. Chem. B **106** (2002) 5143.
7) M. Ohtsu: *Near-field Nano/Atom Optics and Technology* (Springer-Verlag, Tokyo, 1998).
8) J. K. Trautman and J. J. Macklin: Chem. Phys. **205** (1996) 221.
9) B. Knoll and F. Keilmann: Nature **399** (1999) 134.
10) B. Dragnea, J. Preusser, W. Schade, S. R. Leone and W. D. Hinsberg: J. Appl. Phys. **86** (1999) 2795.
11) R. D. Schaller, J. Ziegelbauer, L. F. Lee, L. H. Haber and R. J. Saykally: J. Phys. Chem. B **106** (2002) 8489.
12) R. D. Schaller and R. J. Saykally: Langmuir **17** (2001) 2055.
13) J. D. McNeill, D. B. O'Connor, D. M. Adams, P. F. Barbara and S. B. Kammer: J. Phys. Chem. B **105** (2001) 76.
14) E. J. Ayars and H. D. Hallen: Appl. Phys. Lett. **76** (2000) 3911.
15) L. F. Lee, A. Adronov, R. D. Schaller, J. M. J. Frechet and R. J. Saykally: J. Am. Chem. Soc. **125** (2003) 536.
16) T.-Q. Nguyen, B. J. Schwartz, R. D. Schaller, J. C. Johnson, L. F. Lee, L. H. Haber and R. J. Saykally: J. Phys. Chem. B **105** (2001) 5153.
17) R. D. Schaller, L. F. Lee, J. C. Johnson, L. H. Haber, R. J. Saykally, T.-Q. Nguyen and B. J. Schwartz: J. Phys. Chem. B **106** (2002) 9496.
18) Y. R. Shen: *The Principles of Nonlinear Optics* (J. Wiley, New York, 1984).
19) R. W. Boyd: *Nonlinear Optics* (Academic Press, Boston, 1992).
20) R. D. Schaller, J. C. Johnson and R. J. Saykally: Anal. Chem. **72** (2000) 5361.
21) R. D. Schaller, P. T. Snee, J. C. Johnson, L. F. Lee, K. R. Wilson, L. H. Haber, R. J. Saykally, T.-Q. Nguyen and B. J. Schwartz: J. Chem. Phys. **117** (2002) 6688.
22) T.-Q. Nguyen, I. B. Martini, J. Liu and B. J. Schwartz: J. Phys. Chem. B **104** (2000) 237.
23) T.-Q. Nguyen, V. Doan and B. J. Schwartz: J. Chem. Phys. **110** (1999) 4068.
24) T.-Q. Nguyen, R. C. Kwong, M. E. Thompson and B. J. Schwartz: Appl. Phys. Lett. **76** (2000) 2454.
25) P. Hoffmann, B. Dutoit and R. P. Salathe: Ultramicroscopy **61** (1995) 165.
26) S. L. Gilat, A. Adronov and J. M. J. FrDhet: Angew. Chem. Int. Ed. **18** (1999) 1422.
27) J. M. Lupton, I. D. W. Samuel, R. Beavington, M. J. Frampton, P. L. Burn and H. Bassler: Phys. Rev. B **63** (2001) 155206/1.
28) L.-O. Palsson, R. Beavington, M. J. Frampton, J. M. Lupton, S. W. Magennis, J. P. J. Markham, J. N. G. Pillow, P. L. Burn and I. D. W. Samuel: Macromol. **35** (2002) 7891.
29) K. Kamiyama, M. Era, T. Tsutsui and S. Saito: Jpn. J. Appl. Phys. **29** (1990) L840.
30) J. Teetsov and D. A. Vanden Bout: Langmuir **18** (2002) 897.
31) B. J. Schwartz: to be published in Ann. Rev. Phys. Chem.